Model 920D Scanning Electrochemical Microscope

Overview

The scanning electrochemical microscope (SECM) was introduced in 1989[1] as an instrument that could examine chemistry at high resolution near interfaces. By detecting reactions that occur at a small electrode (the tip) as it is scanned in close proximity to a surface, the SECM can be employed to obtain chemical reactivity images of surfaces and quantitative measurements of reaction rates. Numerous studies with the SECM have now been reported from a number of laboratories all over the world, and the instrument has been used for a wide range of applications, including studies of corrosion, biological systems (e.g., enzymes, skin, leaves), membranes, and liquid/liquid interfaces.[2,3] Trapping and electrochemical detection of single molecules with the SECM has also been reported.

The CHI920D Scanning Electrochemical Microscope consists of a digital function generator, a bipotentiostat, high resolution data acquisition circuitry, a three dimensional nanopositioner, and a sample and cell holder. Diagrams for the SECM and cell/sample holder are shown below. The three dimensional nanopositioner has a spatial resolution down to nanometers but it allows a maximum traveling distance of 50 millimeters. The potential control range of the bipotentiostat is ± 10 V and the current range is ± 250 mA. The instrument is capable of measuring current down to sub-picoamperes.

In addition to SECM imaging, other modes of operation are available for scanning probe applications: Probe Scan Curve, Probe Approach Curve, Surface Interrogation SECM, and Surface Patterned Conditioning. Probe Scan Curve mode allows the probe to move in the X, Y, or Z direction while the probe and substrate potentials are controlled and currents are measured. The probe can be stopped when the current reaches a specified level. This is particularly useful for searching for an object on the surface and determining approach curves. Probe Approach Curve mode allows the probe to approach the surface of the substrate. It is also very useful for distinguishing the surface process using PID control. The step size is automatically adjusted to allow fast surface approach, without letting the probe touch the surface. Surface Patterned Conditioning allows the user to edit a pattern for surface conditioning by controlling the tip at two different potentials and durations. Constant height, constant current, potentiometric, and impedance modes are available for SECM imaging and probe scan curve.

The 920D can do everything the **760E** can do, and more. The 920D is designed for scanning electrochemical microscopy, but many conventional electrochemical techniques have also been integrated for convenience, such as CV, LSV, CA, CC, DPV, NPV, SWV, ACV, SHACV, FTACV, i-t, DPA, DDPA, TPA, SSF, STEP, IMP, IMPE, IMPT, and CP. When the instrument is used as a bipotentiostat, the second channel can be controlled at an independent constant potential, to scan or step at the same potential as the first channel, or to scan with a constant potential difference with the first channel. The second channel works with CV, LSV, CA, DPV, NPV, DNPV, SWV, and i-t.

The 920D SECM is the latest upgrade to the 900 series SECM. The 920D uses a stepper motor positioner in conjunction with a closed-loop 3-dimensional piezo positioner. The stepper motor positioner has a resolution of 8 nanometers with 50 mm travel distance. Closed-loop piezo control allows improved linearity and reduced hysteresis of the piezo devices. Improvements include very stable and accurate potential and current control, and dual-channel data acquisition at high speed (1 MHz with 16-bit resolution).

1. A. J. Bard, F.-R. F. Fan, J. Kwak, and O. Lev, *Anal. Chem*. **61**, 132 (1989); U.S. Patent No. 5,202,004 (April 13, 1993).
2. A. J. Bard, F.-R. Fan, M. V. Mirkin, in *Electroanalytical Chemistry,* A. J . Bard, Ed., Marcel Dekker, New York, 1994, Vol. 18, pp 243-373.
3. A. J. Bard and M. V. Mirkin, Eds. *Scanning Electrochemical Microscopy*, Marcel Dekker, New York, 2001.

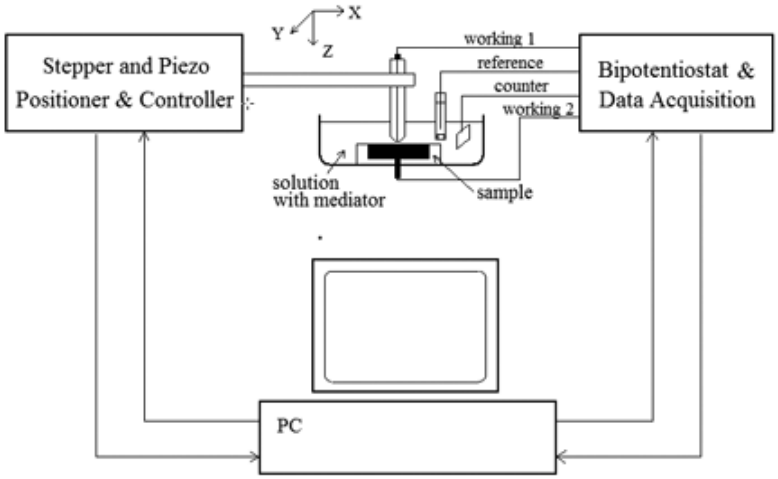

Diagram of Scanning Electrochemical Microscope

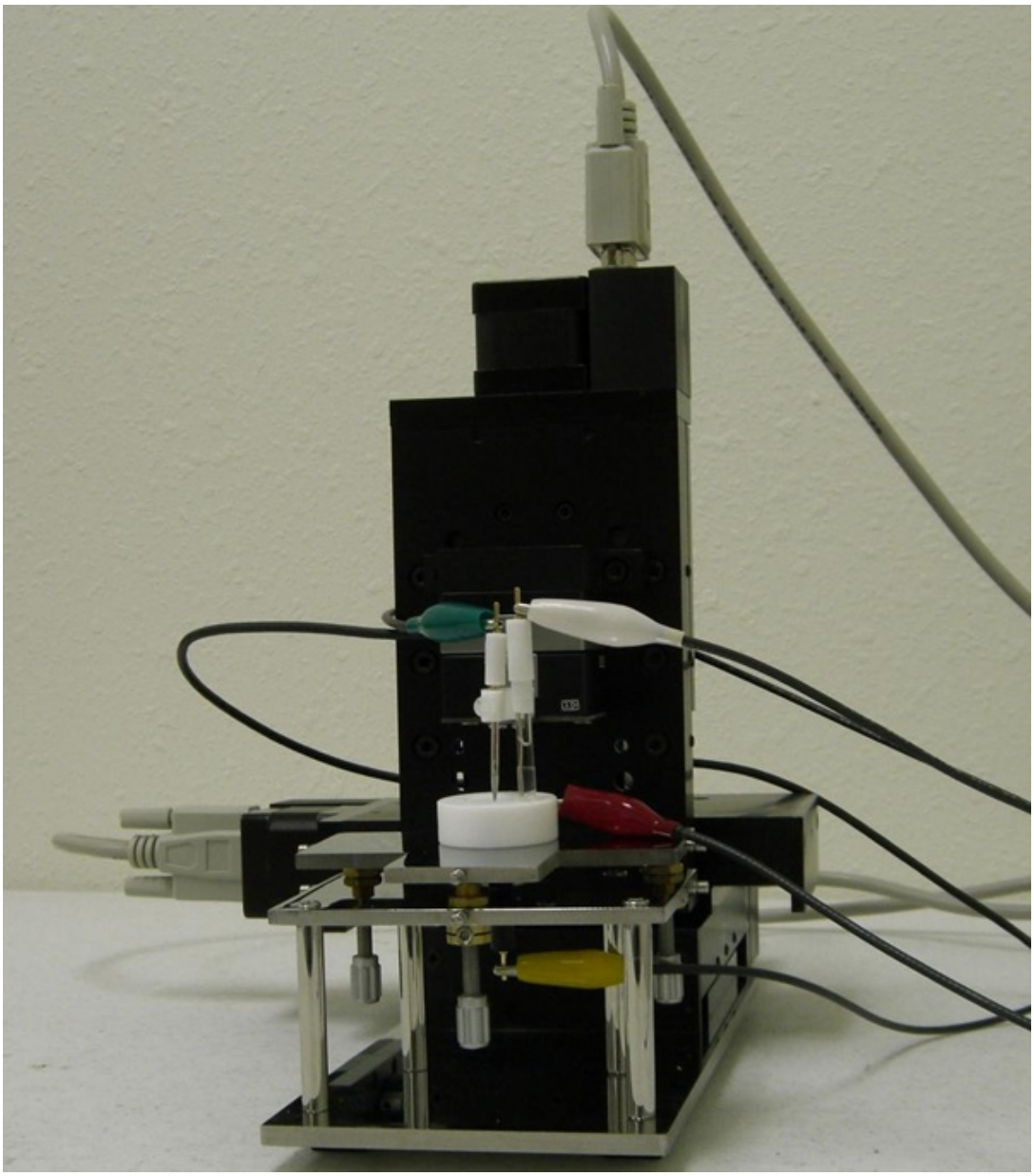

Cell/Sample Holder

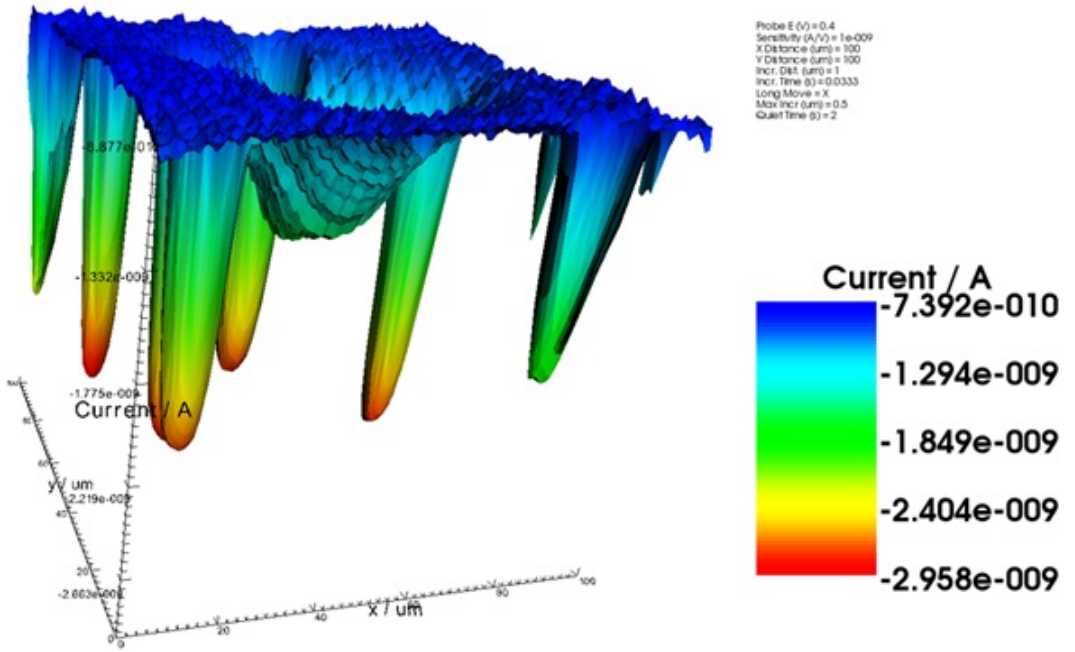

14 µm pore membrance with 2 µm tip

Specifications

Model 920D Series Specifications - for older models (920C, etc.), contact us.

Nanopositioner
- X, Y, Z resolution: 1.6 nm with Piezo positioner, closed loop control, 8 nm with stepper motor positioner
- X, Y, Z total distance: 50 mm

Potentiostat / Bipotentiostat
- Zero resistance ammeter
- 2- or 3- or 4-electrode configuration
- Floating (isolated from earth) or earth ground
- Maximum potential: ±10 V for both channels
- Maximum current: ±250 mA continuous (sum of two current channels), ±350 mA peak
- Compliance Voltage: ±13 V
- Potentiostat rise time: < 1 µs, 0.8 µs typical
- Applied potential ranges (volts): ±0.01, ±0.05, ±0.1, ±0.65, ±3.276, ±6.553, ±10
- Applied potential resolution: 0.0015% of potential range
- Applied potential accuracy: ±1 mV, ±0.01% of scale
- Applied potential noise: < 10 µV rms
- Measured current range: ±10 pA to ±0.25 A in 12 ranges
- Measured current resolution: 0.0015% of current range, minimum 0.3 fA
- Current measurement accuracy: 0.2% if current range >=1e-6 A/V, 1% otherwise
- Input bias current: < 20 pA

Galvanostat
- Galvanostat applied current range: 3 nA - 250 mA
- Applied current accuracy: 20 pA ±0.2% if > 3e-7A, ±1% otherwise
- Applied current resolution: 0.03% of applied current range
- Measured potential range (volts): ±0.025, ±0.1, ±0.25, ±1, ±2.5, ±10
- Measured potential resolution: 0.0015% of measured range

Electrometer
- Reference electrode input impedance: $1x10^{12}$ ohm
- Reference electrode input bandwidth: 10 MHz
- Reference electrode input bias current: <= 10 pA @ 25°C

Waveform Generation and Data Acquisition
- Fast waveform update: 10 MHz @ 16-bit
- Fast data acquisition: dual channel 16-bit ADC, 1,000,000 samples/sec simultaneously
- External signal recording channel at maximum 1 MHz sampling rate

Other Features
- Automatic and manual iR compensation
- Current measurement bias: full range with 16-bit resolution, 0.003% accuracy
- Potential measurement bias: ±10 V with 16-bit resolution, 0.003% accuracy
- External potential input
- Potential and current analog output
- Programmable potential filter cutoff: 1.5 MHz, 150 KHz, 15 KHz, 1.5 KHz, 150 Hz, 15 Hz, 1.5 Hz, 0.15 Hz
- Programmable signal filter cutoff: 1.5 MHz, 150 KHz, 15 KHz, 1.5 KHz, 150 Hz, 15 Hz, 1.5 Hz, 0.15 Hz
- RDE control output: 0-10 V (corresponding to 0-10000 rpm), 16-bit, 0.003% accuracy
- Digital input/output lines programmable through macro command
- Flash memory for quick software update
- Serial port or USB selectable for data communication
- Cell control: purge, stir, knock
- Maximum data length: 256K-16384K selectable
- Real Time Absolute and Relative Distance Display
- Real Time Probe and Substrate Current Display
- Dual-channel measurements for CV, LSV, CA, DPV, NPV, SWV, i-t
- CV simulation and fitting program, user-defined mechanisms
- Impedance simulation and fitting program

Scanning Probe Techniques
- SECM Imaging (SECM): constant height, constant current, potentiometric and impedance modes
- Probe Approach Curves (PAC)
- Probe Scan Curve (PSC): constant height, constant current, potentiometric, impedance, and constant impedance modes
- Surface Patterned Conditioning (SPC)
- Surface Interrogation SECM (SISECM)
- Z Probe Constant Current Control

Sweep Techniques
- Cyclic Voltammetry (CV)
- Linear Sweep Voltammetry
- Tafel Plot (TAFEL)

Step and Pulse Techniques
- Staircase Voltammetry (SCV)
- Chronoamperometry (CA)
- Chronocoulometry (CC)
- Differential Pulse Voltammetry (DPV)
- Normal Pulse Voltammetry (NPV)
- Differential Normal Pulse Voltammetry (DNPV)
- Square Wave Voltammetry

AC Techniques
- AC Voltammetry (ACV)
- Second Harmonic AC Voltammetry (SHACV)
- Fourier Transform AC Voltammetry (FTACV)
- AC Impedance (IMP)
- Impedance versus Potential (IMPE)
- Impedance versus Time (IMPT)

Galvanostatic Techniques
- Chronopotentiometry (CP)
- Chronopotentiometry with Current Ramp (CPCR)
- Multi-Current Steps

Other Techniques
- Amperometric i-t Curve (i-t)
- Differential Pulse Amperometry (DPA)
- Double Differential Pulse Amperometry (DDPA)
- Triple Pulse Amperometry (TPA)
- Integrated Pulse Amperometric Detection (IPAD)
- Bulk Electrolysis with Coulometry (BE)
- Hydrodynamic Modulation Voltammetry (HMV)
- Sweep-Step Functions (SSF)
- Multi-Potential Steps (STEP)
- Electrochemical Noise Measurement (ECN)
- Open Circuit Potential - Time (OCPT)
- Various Stripping Voltammetry
- Potentiometry

Experimental Parameters
- CV and LSV scan rate: 0.000001 to 10,000 V/s, two channels simultaneously
- Potential increment during scan: 0.1 mV @ 1,000 V/s
- CA and CC pulse width: 0.0001 to 1000 sec
- CA minimum sample interval: 1 µs, both channels
- CC minimum sample interval: 1 µs
- True integrator for CC
- DPV and NPV pulse width: 0.001 to 10 sec
- SWV frequency: 1 Hz to 100 kHz
- i-t sample interval: minimum 1 µs, both channels
- ACV frequency: 0.1 Hz to 10 kHz
- SHACV frequency: 0.1 Hz to 5 kHz
- FTACV frequency: 0.1 Hz to 50 Hz, simultaneously acquire 1st, 2nd, 3rd, 4th, 5th, and 6th harmonics ACV data
- IMP frequency: 0.00001 Hz to 1 MHz
- IMP amplitude: 0.00001 V to 0.7 V rms

2D and 3D Graphics:
- Interactive visualization of SECM surfaces
- Color mapping
- Laplacian smoothing
- Stereoscopic 3D anaglyph imaging
- High compatibility: Windows 98 and up, 256 colors (VGA) and up, no special video card or display required

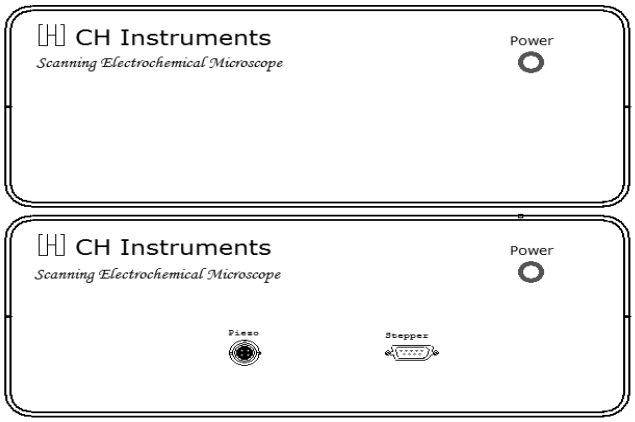

Front View of Bipotentiostat (top) and Motor Controller (bottom)

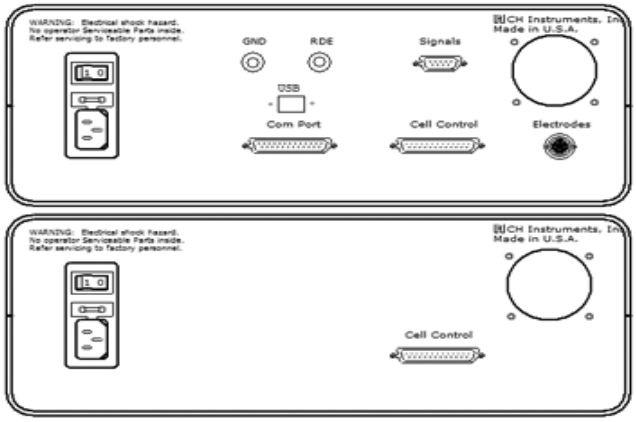

Rear View of Bipotentiostat (top) and Motor Controller (bottom)

Techniques

Scanning Probe Techniques

- SECM Imaging (SECM): constant height, constant current, potentiometric, and impedance modes
- Probe Approach Curves (PAC)
- Probe Scan Curve (PSC) : constant height, constant current, potentiometric, and impedance modes
- Surface Patterned Conditioning (SPC)
- Surface Integration SECM (SISECM)

Sweep Techniques

- Cyclic Voltammetry (CV)
- Linear Sweep Voltammetry (LSV)
- Tafel Plot (TAFEL)

Step and Pulse Techniques

- Staircase Voltammetry (SCV)
- Chronoamperometry (CA)
- Chronocoulometry (CC)
- Differential Pulse Voltammetry (DPV)
- Normal Pulse Voltammetry (NPV)
- Differential Normal Pulse Voltammetry (DNPV)
- Square Wave Voltammetry (SWV)

AC Techniques

- AC Voltammetry (ACV)
- Second Harmonic AC Voltammetry (SHACV)
- AC Impedance (IMP)
- Impedance versus Potential (IMPE)
- Impedance versus Time (IMPT)

Galvanostatic Techniques

- Chronopotentiometry (CP)
- Chronopotentiometry with Current Ramp (CPCR)
- Multi-Current Steps (ISTEP)
- Potentiometric Stripping Analysis (PSA)

Other Techniques

- Amperometric i-t Curve (i-t)
- Differential Pulse Amperometry (DPA)
- Double Differential Pulse Amperometry (DDPA)
- Triple Pulse Amperometry (TPA)
- Integrated Pulse Amperometric Detection (IPAD)
- Bulk Electrolysis with Coulometry (BE)
- Hydrodynamic Modulation Voltammetry (HMV)
- Sweep-Step Functions (SSF)
- Multi-Potential Steps (STEP)
- Electrochemical Noise Measurements (ECN)
- Open Circuit Potential - Time (OCPT)
- Various Stripping Voltammetry
- Potentiometry

Principles and Applications

Download SECM Brochure (PDF)

Example Applications

- Electrode surface studies
- Corrosion
- Biological samples
- Solid dissolution
- Liquid/liquid interfaces
- Membranes

I. Operational Principles of SECM

As in other types of scanning probe microscopy, SECM is based on the movement of a very small electrode (the tip) near the surface of a conducting or insulating substrate.[1] In amperometric SECM experiments, the tip is usually a conventional ultra-microelectrode (UME) fabricated as a conductive disk of metal or carbon in an insulating sheath of glass or polymer. Potentiometric SECM experiments with ion-selective tips are also possible.[2]

In amperometric experiments, the tip current is perturbed by the presence of the substrate. When the tip is far (i.e. greater than several tip diameters) from the substrate, as shown in Fig. 1A, the steady-state current, $i_{T,\infty}$, is given by

$$i_{T,\infty} = 4nFDCa$$

where F is Faraday's constant, n is the number of electrons transferred in the tip reaction (O + ne → R), D is the diffusion coefficient of species O, C is the concentration, and a is the tip radius. When the tip is moved toward the surface of an insulating substrate, the tip current i_T decreases because the insulating sheath of the tip blocks diffusion of O to the tip from the bulk solution. The closer the tip gets to the substrate, the smaller i_T becomes (Fig 1b). On the other hand, with a conductive substrate, species R can be oxidized back to O. This produces an additional flux of O to the tip and hence an increase in i_T (Fig. 1c). In this case, the smaller the value of D, the larger i_T will be, with $i_T \rightarrow \infty$ as $D \rightarrow 0$, assuming the oxidation of R on the substrate is diffusion-limited. These simple principles form the basis for the feedback mode of SECM operation.

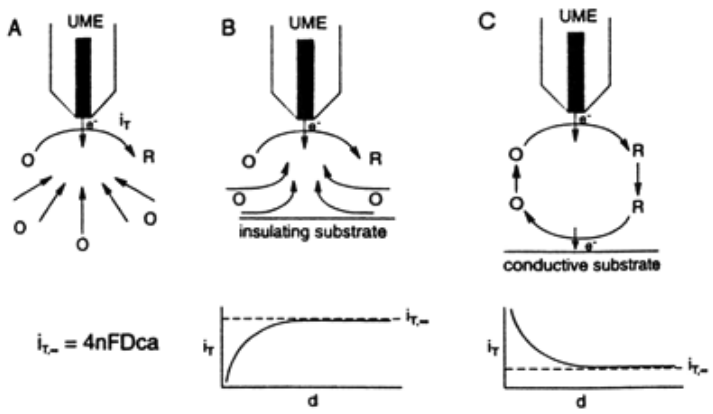

Figure 1. *Operating principles of SECM. (a) With the UME far from the substrate, diffusion of O leads to a steady-state current, $i_{T,\infty}$. (b) With the UME placed near an insulating substrate, hindered diffusion of O leads to $i_T < i_{T,\infty}$. (c) With the UME near a conducting substrate, positive feedback of O leads to $i_T > i_{T,\infty}$.*

When the tip is rastered in the x-y plane above the substrate, the tip current variation represents changes in topography or conductivity (or reactivity). One can separate topographic effects from conductivity effects by noting that over an insulator i_T is always less than $i_{T,\infty}$, while over a conductor i_T is always greater than $i_{T,\infty}$.

In the feedback mode of the SECM operation mentioned above, the overall redox process is essentially confined to the thin layer between the tip and the substrate. In the substrate-generation/tip-collection (SG/TC) mode (when the substrate is a generator and the tip is a collector), the tip travels within a thin diffusion layer generated by the substrate electrode.[1b,3] There are some shortcomings which limit the applicability of the SG/TC mode if the substrate is large: (1) the process at a large substrate is always non-steady state; (2) a large substrate current may cause significant iR-drop; and (3) the collection efficiency, i.e., the ratio of the tip current to the substrate current, is low. The tip-generation/substrate-collection (TG/SC) mode is advisable for kinetic measurements, while SG/TC can be used for monitoring enzymatic reactions, corrosion, and other heterogeneous processes at the substrate surface.

II. Applications

A. Imaging and positioning

A three-dimensional SECM image is obtained by scanning the tip in the x-y plane and monitoring the tip current, i_T, as a function of tip location.

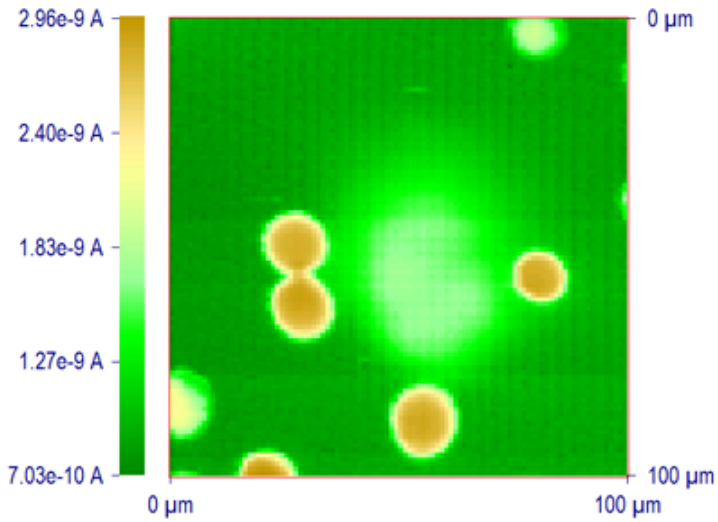

Figure 2. *SECM image of a polycarbonate filtration membrane with a 2 µm diameter Pt disk UME in $Fe(CN)_6^{4-}$ solution. Average pore diameter is ca. 10 µm.*

A particular advantage of SECM in imaging applications, compared to other types of scanning probe microscopy, is that the response observed can be interpreted based on fairly rigorous theory, and hence the measured current can be employed to estimate the tip-substrate distance. Moreover, SECM can be used to image the surfaces of different types of substrates, both conductors and insulators, immersed in solutions. The resolution attainable with SECM depends upon the tip radius. For example, Fig. 2 shows one SECM image of a filtration membrane obtained with a 2 µm diameter Pt disk tip in $Fe(CN)_6^{4-}$ solution. Average pore diameter is ca. 10 µm. An image demonstrating the local activity of an enzymatic reaction on a filtration membrane is shown in Fig. 9 as described below.

B. Studies of heterogeneous electron transfer reactions

SECM has been employed in heterogeneous kinetic studies on various metal, carbon and semiconductor substrates.[4] In this application, the x-y scanning feature of SECM is usually not used. In this mode, SECM has many features of UME and thin layer electrochemistry with a number of additional advantages. For example, the characteristic flux to an UME spaced a distance d from a conductive substrate is of the order of DC/d, independent of the tip radius a when d < a. Thus, very high fluxes and thus high currents can be obtained. For example, the measurement of the very fast kinetics of the oxidation of ferrocene at a Pt UME has been carried out.[4e] Five steady-state voltammograms obtained at different distances are shown in Fig. 3, along with theoretical curves calculated with the values of kinetic parameters extracted from quartile potentials. The heterogeneous rate constant k^o obtained (3.7 ± 0.6 cm/sec) remains constant within the range of experimental error, while the mass-transfer rate increases with a decrease in d.

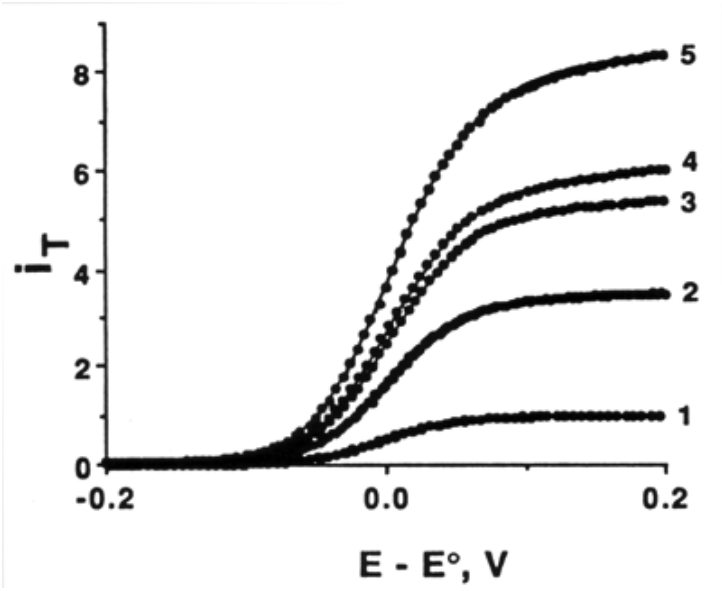

Figure 3. *Tip steady-state voltammograms for the oxidation of 5.8 mM ferrocene in 0.52 M $TBABF_4$ in MeCN at a 1.1 μm radius Pt tip. Solid lines are theoretical curves and solid circles are experimental data. Tip-substrate separation decreases from curve 1 to 5 (d/a = ∞, 0.27, 0.17, 0.14, and 0.1). (Reprinted with permission from Ref. 4e, © 1993, American Chemical Society.)*

C. Studies of homogeneous chemical reactions

In the same manner as the rotating ring disk electrode (RRDE), the TG/SC mode of SECM described above (with small tip and substrate), is particularly well suited to the studies of homogeneous chemical kinetics.[1b,5] The SECM approach has the additional advantage that different substrates can be examined easily, i.e., without the need to construct RRDEs that can be rather difficult to fabricate, and higher interelectrode fluxes are available without the need to rotate the electrode or otherwise cause convection in the solution. Moreover, in the TG/SC mode, the collection efficiency in the absence of perturbing homogeneous chemical reactions is near 100%, compared to significantly lower values in practical RRDEs. Finally, although transient SECM measurements are possible, most reported applications have involved steady-state currents, which are easier to measure, are not perturbed by factors like double-layer charging, and also allow for signal averaging. For example, the reductive coupling of both dimethyl-fumarate (DF) and fumaronitrile (FN) in N,N-dimethyl formamide has been studied with the TG/SC mode.[5a] Fig. 4 shows tip and substrate steady-state voltammograms in the TG/SC regime. Comparable values of both of the plateau currents indicate that the mass transfer rate was sufficiently fast to study the rapid homogeneous reaction. From the approach curves of tip and substrate currents obtained at various FN concentrations (Fig. 5), a rate constant k_c = 2.0 (± 0.4) x 10^5 $M^{-1}s^{-1}$ was determined for the dimerization reactions.

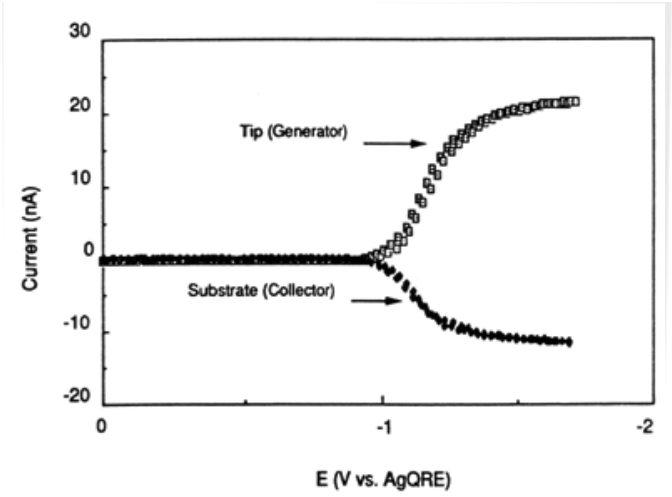

Figure 4. *SECM voltammograms for FN (28.2 mM) reduction in TG/SC mode, with d = 1.8 μm. E_T was scanned at 100 mV/sec with E_S = 0.0 V vs AgQRE. (Reprinted with permission from Ref. 5a, copyright 1992, American Chemical Society.)*

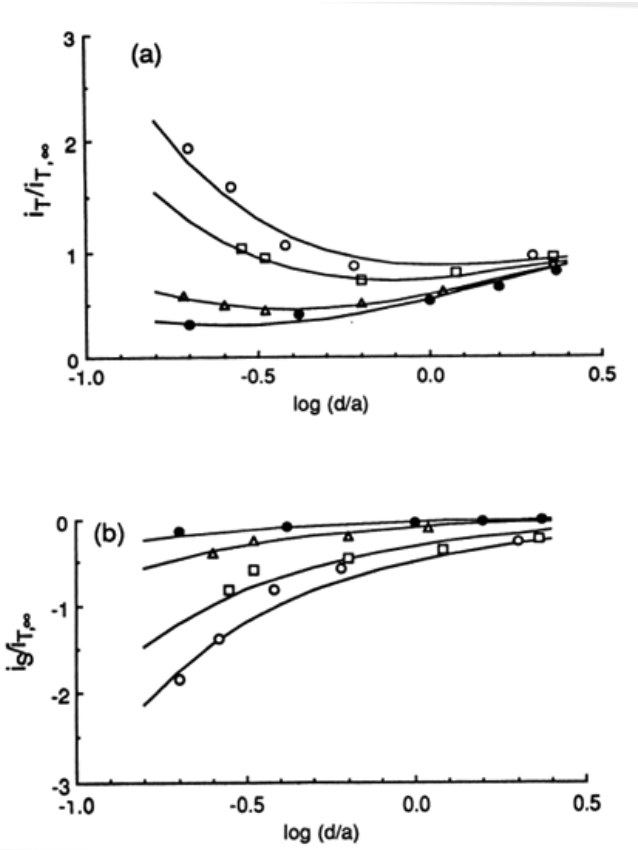

Figure 5. *(a) Normalized tip (generation) and (b) substrate (collection) current-distance behavior for FN reduction. FN concentration: (open circles) 1.50 mM, (open squares) 4.12 mM, (open triangles) 28.2 mM, and (filled circles) 121 mM. The tip radius a = 5 μm and the substrate radius is 50 μm. The solid lines represent the best theoretical fit for each set of data. (Reprinted with permission from Ref. 5a, copyright 1992, American Chemical Society.)*

D. Characterization of thin films and membranes

SECM is also a useful technique for studying thin films on interfaces. Both mediated and direct electrochemical measurements on thin films or membranes can be carried out. For example, polyelectrolytes, electronically conductive polymers, passivation films on metals, and dissolution processes have been investigated by SECM.[6] A unique type of cyclic voltammetry, called tip-substrate cyclic voltammetry (T/S CV), has been used to investigate the electrochemical behavior of an $Os(bpy)_3^{2+}$-incorporated Nafion film.[6a] T/S CV involves monitoring the tip current vs. the substrate potential (E_S) while the tip potential (ET) is maintained at a given value and the tip is held near the substrate. The substrate CV (i_S vs. E_S) of an $Os(bpy)_3^{2+}$-incorporated Nafion film covering a Pt disk electrode in $Fe(CN)_6^{3-}$ solution only shows a wave for the $Os(bpy)_3^{2+/3+}$ couple (Fig. 6B), indicating the permselectivity of the Nafion coating. Fig. 6A shows the corresponding T/S CV curves. When the tip is far from the substrate, i_T is essentially independent of E_S. When the tip is close to the substrate (d = 10 μm), either negative or positive feedback effects are observed, depending on the oxidation state of the $Os(bpy)_3^{2+/3+}$ couple in the Nafion. When E_S is swept positive of the $Os(bpy)_3^{2+/3+}$ redox wave, a positive feedback effect is observed due to the regeneration of $Fe(CN)_6^{3-}$ in the solution gap region because of the oxidation of $Fe(CN)_6^{4-}$ by $Os(bpy)_3^{3+}$ at the solution-film interface. When E_S is negative of the redox wave, the film shows negative feedback behavior, since the $Os(bpy)_3^{2+}$ formed is unable to oxidize tip-generated $Fe(CN)_6^{4-}$ back to $Fe(CN)_6^{3-}$.

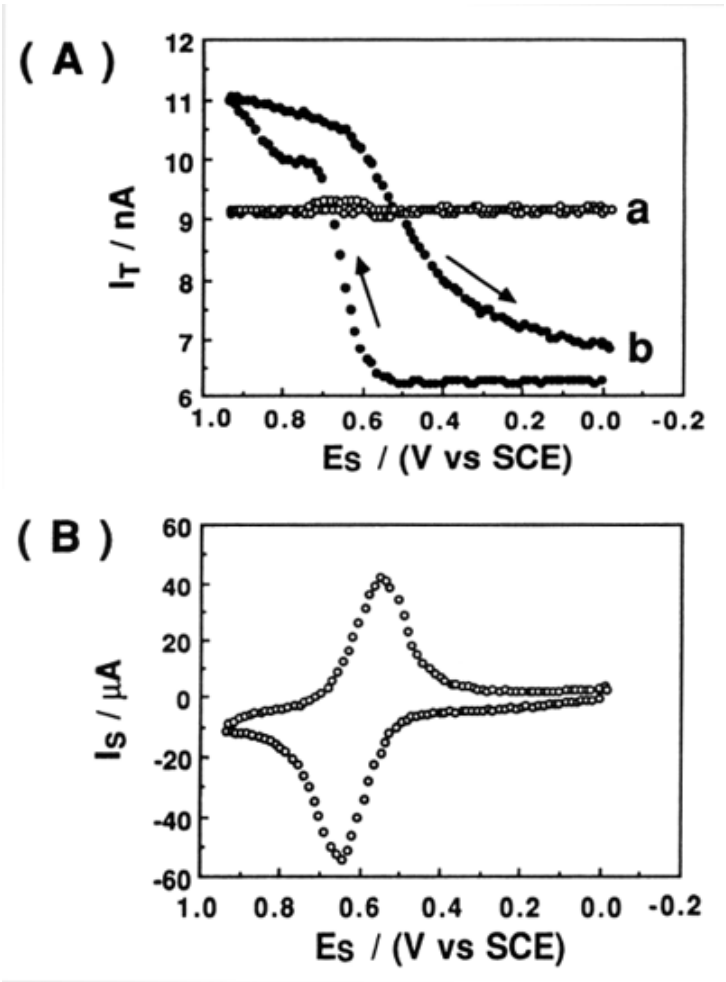

Figure 6. *(A) T/S CVs curve a, d = 500 µm, (B) substrate CV on Nafion/Os(bpy)$_3^{3+/2+}$ electrode in $K_3Fe(CN)_6/Na_2SO_4$, scan rate = 50 mV/sec, E_T = -0.4 V vs. SCE. (Reprinted with permission from Ref. 6a, copyright 1990, American Chemical Society.)*

E. Liquid-liquid interfaces

One of the most promising applications of SECM is the study of charge transport at the interface between two immiscible electrolyte solution (ITIES).[7] Unlike conventional techniques, SECM allows for the studies of both ion and electron transfer at the interface. For example, uphill electron transfer, in which an electron is transferred uphill from a redox couple with a higher standard reduction potential in one phase to another redox couple having a lower standard reduction potential in a second immiscible phase has been demonstrated using the system TCNQ (in 1,2-dichroloethane [DCE])/ferrocyanide (in water).[7c] Fig. 7 shows the approach curve obtained as the UME approaches the interface when the system contains supporting electrolytes with no partitioning ions such as tetraphenylarsonium ($TPAs^+$). However, the reverse electron flow for the same redox reaction can be induced by employing TPA^+ as a potential-determining ion as shown in Fig. 8. The driving force for this reverse electron transfer is the imposition of an interfacial potential difference by the presence in solution of TPA^+ in both phases ($\Delta_{owφ}$ = -364 mV). Note that the detection of reverse electron flow in this case could not be done using methods commonly used for studies of the ITIES, e.g., cyclic voltammetry. Since the ITIES is not polarizable in the presence of TPA^+ in both phases, any attempt to impose externally a potential across the interface with electrodes in two phases would result in interfacial ion transfer and a current flow. The SECM approach does not suffer from this interference. Charge transfer processes across the ITIES with or without membranes have also been studied.

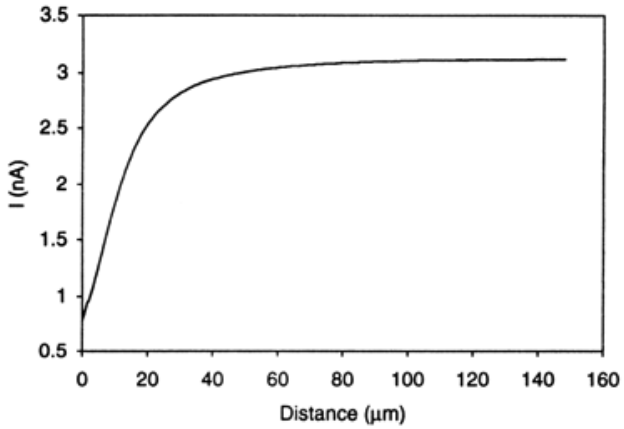

Figure 7. *Approach curve for the system: 10 mM TCNQ and 1 mM TPAsTPB in DCE // 1 mM $Fe(CN)_6^{3-}$ and 0.1 M LiCl in H_2O, showing the absence of electron transfer across the liquid/liquid interface. A 25 µm diameter Pt microelectrode was used to generate $Fe(CN)_6^{4-}$ at the electrode tip from the $Fe(CN)_6^{3-}$. Tip potential, -0.4 V vs Ag/AgCl. (Reprinted with permission from Ref. 7c, copyright 1995, American Chemical Society.)*

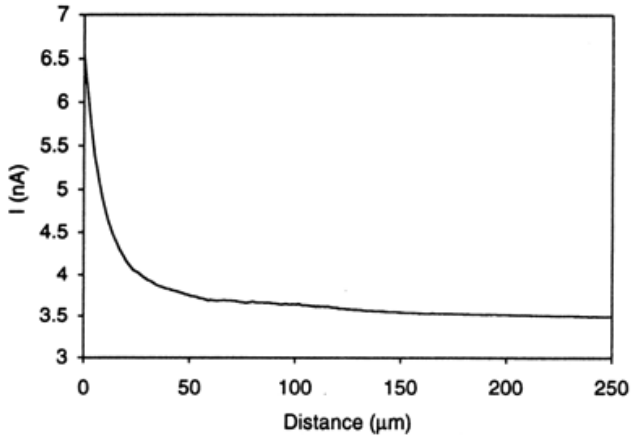

Figure 8. *Approach curve for the system: 10 mM TCNQ and 1 mM TPAsTPB in DCE // 1 mM $Fe(CN)_6^{3-}$, 0.1 M LiCl and 1 mM TPAsCl in H_2O, showing reverse electron transfer driven by the phase transfer catalyst $TPAs^+$. Tip potential, -0.4 V vs Ag/AgCl. (Reprinted with permission from Ref. 7c, copyright 1995, American Chemical Society.)*

F. Probing patterned biological systems

SECM has been actively employed to probe artificially or naturally patterned biological systems.[8] Both amperometric and potentiometric techniques with ion-selective tips can be used. A direct test of the SECM's ability to image an enzymatic reaction over a localized surface region[8a] is shown in Fig. 9. Glucose oxidase (GO) hydrogel was filled inside small, well-defined pores of a polycarbonate filtration membrane. The buffered assay solution contained a high concentration of D-glucose as well as two redox mediators, methyl viologen dication (MV^{2+}) and neutral hydroquinone (H_2Q). Fig. 9a shows an image obtained with a tip potential of -0.95 V vs. a silver quasi reference electrode (AgQRE) where MV^{2+} was reduced to $MV^{+\cdot}$. Since $MV^{+\cdot}$ does not react with reduced GO at the hydrogel-filled region, a negative feedback current was obtained. However, with the tip potential changed to 0.82 V, where hydroquinone was oxidized to p-benzoquinone by reduced GO, an increased tip current was observed (Fig. 9b). This positive feedback current over the hydrogel region indicates a significant catalytic feedback of the hydroquinone and provides a direct image of the local enzymatic reaction.

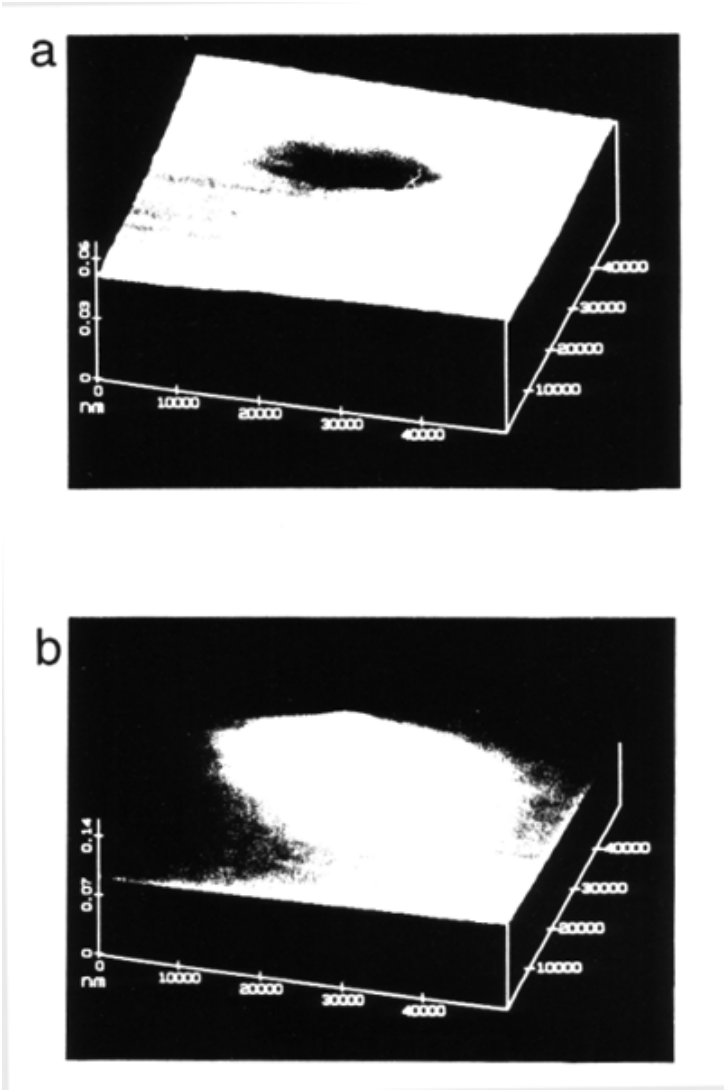

Figure 9. *SECM images (50 μm x 50 μm) of a single GO hydrogel-filled pore on the surface of a treated membrane. Images were taken with a carbon microelectrode tip (a = 4.0 μm). (a) Negative feedback with MV^{2+} mediator at tip potential -0.95 V vs AgQRE. (b) Positive feedback with hydroquinone mediator at tip potential +0.82 V vs AgQRE in 0.1 M phosphate-perchlorate buffer (pH 7.0) containing 100 mM D-glucose, 50 μM hydroquinone and 0.1 mM $MVCl_2$. Lightest image regions depict the greatest tip current. Reprinted with permission from Ref. 8a, copyright 1993, American Chemical Society.)*

G. Fabrication

The SECM can be used to fabricate microstructures on surfaces by deposition of metal or other solids or by etching of the substrate.[9] Two different approaches have been used, direct mode[9a,b] and feedback mode[9c]. Typically, in the direct mode, the tip, held in close proximity to the substrate, acts as a working electrode (in deposition reactions) or as the counterelectrode (in etching processes). The feedback mode of fabrication utilizes the same arrangement as in SECM imaging.

The tip reaction is selected to generate a species that reacts at the substrate to promote the desired reaction, i.e., deposition or etching. For example, a strong oxidant, like Br_2, generated at the tip can etch the area of the substrate, e.g., GaAs, directly beneath the tip.[9d] The mediator reactant is chosen to be one that reacts completely and rapidly at the substrate, thus confining the reaction to a small area on the substrate and producing features of area near that of the tip. Small tip size and close tip-substrate spacing are required for high resolution.

III. References

1. (a). A. J. Bard, F.-R. F. Fan, J. Kwak, and O. Lev, *Anal. Chem*. **1989**, *61*, 132; (b). A. J. Bard, F.-R. F. Fan, and M. V. Mirkin in *Electroanalytical Chemistry*, Vol.18 (A. J. Bard, ed.), Marcel Dekker, New York, 1994, p. 243.
2. e.g., (a). For a review of early potentiometric SECM experiments, see Ref. 1b; (b). C. Wei, A. J. Bard, G. Nagy, and K. Toth, *Anal. Chem*. **1995**, *67*, 1346; (c). K. Toth, G. Nagy, C. Wei, and A. J. Bard, *Electroanal*. **1995**, *7*, 801; (d). M. Kupper and J. W. Schultze, *Fres. J. Anal. Chem*. **1996**, *356*, 187.
3. See also (a). R. C. Engstrom, M. Weber, D. J. Wunder, R. Burgess, and S. Winquist, *Anal. Chem*. **1986**, *58*, 844; (b). R. C. Engstrom, T. Meaney, R. Tople, and R. M. Wightman, *Anal. Chem*. **1987**, *59*, 2005.
4. e.g., (a). D. O. Wipf and A. J. Bard, *J. Electrochem. Soc*. **1991**, *138*, 469; (b). B. R. Horrocks, M. V. Mirkin, and A. J. Bard, *J. Phys. Chem*. **1994**, *98*, 9106; (c). R. S. Hutton and D. E. Williams, *Electrochim. Acta*, **1994**, *39*, 701; (d). N. Casillas, P. James, and W. H. Smyrl, *J. Electrochem. Soc*. **1995**, *142*, L16; (e). M. V. Mirkin, T. C. Richards, and A. J. Bard, *J. Phys. Chem*. **1993**, *97*, 7672; (f). M. V. Mirkin, L.O.S. Bulhoes, and A. J. Bard, *J. Am. Chem. Soc*. **1993**, *115*, 201; (g). J. V. Macpherson, M. A. Beeston, and P. R. Unwin, *J. Chem. Soc. Faraday Trans*. **1995**, *91*, 899.
5. e.g., (a). F. M. Zhou, P. R. Unwin, and A. J. Bard, *J. Phys. Chem*. **1992**, *96*, 4917; (b). P.R. Unwin and A. J. Bard, *J. Phys. Chem*. **1991**, *95*,7814; (c). F. M. Zhou and A. J. Bard, *J. Am Chem. Soc*. **1994**, *116*, 393; (d). D. A. Treichel, M. V. Mirkin, and A. J. Bard, *J. Phys. Chem*. **1994**, *98*, 5751; (e). C. *100*, 17881; (f). C. J. Slevin, J. A. Umbers, J. H. Atherton, and P. R. Unwin, *J. Chem. Soc. Faraday* Demaille, P. R. Unwin, and A. J. Bard, *J. Phys. Chem*. **1996**, *100*, 14137.
6. e.g., (a). C. Lee and A. J. Bard, *Anal. Chem*. **1990**, *62*, 1906; (b). C. Lee, J. Kwak, and F. C. Anson, *Anal. Chem*. **1991**, *63,* 1501; (c). J. Kwak, C. Lee, and A. J. Bard, *J. Electrochem. Soc*. **1990**, *137*, 1481; (d). C. Lee and F. C. Anson, *Anal. Chem*. **1992**, *64*, 250. (e). I. C.

Jeon and F. C. Anson, *Anal. Chem*. **1992**, *64*, 2021; (f). M. V. Mirkin, F.-R. F. Fan, and A. J. Bard, *Science*, **1992**, *257*, 364. (g). M. Arca, M. V. Mirkin, and A. J. Bard, *J. Phys. Chem*. **1995**, *99*, 5040; (h). M. Pyo and A. J. Bard, *Electrochim. Acta* **1997**, *42*, 3077; (i). E. R. Scott, A. I. Laplaza, H. S. White, and J. B. Phipps, *Pharmaceut. Res*. **1993**, *10*, 1699; (j). S. R. Snyder and H. S. White, *J. Electroanal. Chem*. **1995**, *394*, 177; (k). S. B. Basame and H. S. White, *J. Phys. Chem*. **1995**, *99*,16430; (l). N. Casillas, S. Charlebois, W. H. Smyrl, and H. S. White, *J. Electrochem. Soc*. **1994**, *141*, 636; (m). D. O. Wipf, *Colloid Surf. A,* **1994**, *93***,** 251. (n). E. R. Scott, H. S. White, and J. B. Phipps, *Solid State Ionics* **1992**, *53*, 176; (o). S. Nugnes and G. Denuault, *J. Electroanal. Chem*. **1996**, *408*, 125; (p). M. H. T. Frank and G. Denuault, *J. Electroanal. Chem*. **1993**, *354*, 331; (q). J. V. Macpherson and P. R. Unwin, *J. Chem. Soc. Faraday Trans*. **1993**, *89*, 1883; (r). J. V. Macpherson and P. R. Unwin, *J. Phys. Chem*. **1994**, *98*, 1704; (s). J. V. Macpherson and P. R. Unwin. *J Phys. Chem*. **1995**, *99*, 14824; **1996**, *100*, 19475; (t). J. V. Macpherson, C. J. Slevin, and P. R. Unwin*, J. Chem. Soc. Faraday Trans.* **1996**, *92*, 3799; (u). K. Borgwarth, C. Ricken, D. G. Ebling, and Heinze, *Ber. Bunsenges. Phys. Chem*. **1995**, *99*, 1421; (v). Y. Y. Zhu and D. E. Williams, *J. Electrochem. Soc*. **1997**, *144*, L43; (w). C. Jehoulet, Y. S. Obeng, Y. T. Kim, F. M. Zhou, and A. J. Bard, *J. Am. Chem. Soc.* **1992**, *114*, 4237; (x). E. R. Scott, H. S. White, and J. B. Phipps, *J. Membrane Sci.*. **1991**, *58*, 71; (y). H. Sugimura, T. Uchida, N. Kitamura, and H. Masuhara, *J. Phys. Chem*. **1994**, *98*, 4352; (z). J. E. Vitt and R. C. Engstrom, Anal. Chem. **1997**, *69*, 1070.

7. e.g., (a). C. Wei, A. J. Bard, and M. V. Mirkin, *J. Phys. Chem*. **1995**, *99*, 16033; (b). T. Solomon and A. J. Bard, *J. Phys. Chem*. **1995**, *67*, 2787; (c). T. Solomon and A. J. Bard, *J. Phys. Chem*. **1995**, *99*, 17487; (d). Y. Selzer and D. Mandler, *J. Electroanal. Chem*. **1996**, **409**, 15; (e). M. Tsionsky, A. J. Bard, and M. V. Mirkin, *J. Phys. Chem*. **1996**, *Trans*. **1996**, **92**, 5177; (g). Y. H. Shao, M. V. Mirkin, and J. F. Rusling, *J. Phys. Chem. B* **1997**, *101*, 3202; (h). M. Tsionsky, A. J. Bard, and M. V. Mirkin, *J. Am. Chem. Soc.* **1997**, *119*, 10785; (i). M.-H. Delville, M. Tsionsky, and A. J. Bard, (submitted to *J. Am. Chem. Soc*. for publication).
8. e.g., (a). D. T. Pierce and A. J. Bard, *Anal. Chem*. **1993**, *65*, 3598; (b). B. R. Horrocks, D. Schmidtke, A. Heller, and A. J. Bard, *Anal. Chem*. **1993**, *65*, 3605; (c). H. Yamada, H. Shiku, T. Matsue, and I. Uchida, *Bioelectrochem. Bioenerg*. **1994**, *33*, 91; (d). B. Grundig, G. Wittstock, U. Rudel, and B. Strehlitz, *J. Electroanal. Chem*. **1995**, *395*, 143; (e). G. Wittstock, K. J. Yu, H. B. Halsall, T. H. Ridgway, and W. R. Heineman, *Anal. Chem*. **1995**, *67*, 3578; (f). H. Shiku, T. Matsue, and I. Uchida, *Anal. Chem*. **1996**, *68*, 1276; (g). J. L. Gilbert, S. M. Smith, and E. P. Lautenschlager, *J. Biomed. Mater. Res*. **1993**, *27*, 1357; (h). C. Kranz, T. Lotzbeyer, H. L. Schmidt, and W. Schuhmann, *Biosens. Bioelectron*. **1997**, *12*, 257; (i). C. Kranz, G. Wittstock, H. Wohlschlager, and W. Schuhmann, *Electrochim. Acta*, **1997**, *42*, 3105; (j). C. Lee, J. Kwak, and A. J. Bard, *Proc. Natl. Acad. Sci. U.S.A*. **1990**, *87*, 1740; (k). R. B. Jackson, M. Tsionsky, Z. G. Cardon, and A. J. Bard, *Plant Physiol*. **1996**, *112*, 354; (l). M. Tsionsky, Z. G. Cardon, A. J. Bard, and R. B. Jackson, *Plant Physiol*. **1997**, *113*, 895.
9. e.g., (a). C. W. Lin, F.-R. F. Fan, and A. J. Bard, *J. Electrochem. Soc*. **1987**, *134*, 1038; (b). D. H. Craston, C. W. Lin, and A. J. Bard, *J. Electrochem. Soc*. **1988**, *135*, 785; (c). D. Mandler and A. J. Bard, *J. Electrochem. Soc*. **1989**, *136*, 3143; (d). D. Mandler and A. J. Bard, *J. Electrochem. Soc*. **1990**, *137*, 2468; (e). O. E. Husser, D. H. Craston, and A. J. Bard. *J. Vac. Sci. Technol. B* **1988**, *6*, 1873; (f). Y.-M. Wuu, F.-R. F. Fan, and A. J. Bard, *J. Electrochem. Soc*. **1989**, *136*, 885; (g). H. Sugimura, T. Uchida, N. Shimo, N. Kitamura, and H. Masuhara, *Ultramicroscopy* **1992**, *42*, 468; (h). I. Shohat and D. Mandler, *J. Electrochem. Soc*. **1994**, *141*, 995; (i). S. Meltzer and D. Mandler, *J. Chem. Soc. Faraday Trans*. **1995**, *91*, 1019; (j). C. Kranz, H. E. Gaub, and W. Schuhmann, *Advan. Mater*. **1996**, *8*, 634; (k). J. F. Zhou and D. O. Wipf, *J. Electrochem. Soc*. **1997**, *144*, 1202.

Order SECM